RESEARCH PAPER

Sleep patterns in Parkinson's disease: direct recordings from the subthalamic nucleus

John A Thompson,[1] Anand Tekriwal,[2] Gidon Felsen,[3] Musa Ozturk,[4] Ilknur Telkes,[4] Jiangping Wu,[5] Nuri Firat Ince,[4] Aviva Abosch[2]

[1]Department of Neurosurgery, University of Colorado School of Medicine, Aurora, Colorado, USA
[2]Medical Scientist Training Program, University of Colorado School of Medicine, Aurora, Colorado, USA
[3]Department of Physiology and Biophysics, University of Colorado School of Medicine, Aurora, Colorado, USA
[4]Biomedical Engineering, University of Houston, Texas, USA
[5]Neuromodulation Global Research, Medtronic, Minneapolis, Minnesota, USA

Correspondence to
Dr John A Thompson, Department of Neurosurgery, University of Colorado School of Medicine, Aurora, CO 80045, USA; john.a.thompson@ucdenver.edu

JAT and AT contributed equally.

Received 23 March 2017
Revised 13 August 2017
Accepted 14 August 2017
Published Online First 2 September 2017

ABSTRACT

Sleep is a fundamental homeostatic process, and disorders of sleep can greatly affect quality of life. Parkinson's disease (PD) is highly comorbid for a spectrum of sleep disorders and deep brain stimulation (DBS) of the subthalamic nucleus (STN) has been reported to improve sleep architecture in PD. We studied local field potential (LFP) recordings in PD subjects undergoing STN-DBS over the course of a full-night's sleep. We examined the changes in oscillatory activity recorded from STN between ultradian sleep states to determine whether sleep-stage dependent spectral patterns might reflect underlying dysfunction. For this study, PD (n=10) subjects were assessed with concurrent polysomnography and LFP recordings from the DBS electrodes, for an average of 7.5 hours in 'off' dopaminergic medication state. Across subjects, we found conserved spectral patterns among the canonical frequency bands (delta 0–3 Hz, theta 3–7 Hz, alpha 7–13 Hz, beta 13–30 Hz, gamma 30–90 Hz and high frequency 90–350 Hz) that were associated with specific sleep cycles: delta (0–3 Hz) activity during non-rapid eye movement (NREM) associated stages was greater than during Awake, whereas beta (13–30 Hz) activity during NREM states was lower than Awake and rapid eye movement (REM). In addition, all frequency bands were significantly different between NREM states and REM. However, each individual subject exhibited a unique mosaic of spectral interrelationships between frequency bands. Our work suggests that LFP recordings from human STN differentiate between sleep cycle states, and sleep-state specific spectral mosaics may provide insight into mechanisms underlying sleep pathophysiology.

INTRODUCTION

Sleep is a fundamental biological process crucial to homeostasis.[1 2] Given the complex nature of sleep as a behavioural, neurological and physiological state, dysregulation can arise from several sources.[2] Consequently, sleep dysfunction has been classified into over 80 distinct disorders and is prevalent in the US adult population (>50 million[3]) and exerts a high cost on quality of life, productivity and healthcare.[4–6]

Our knowledge of human sleep has largely been informed by electroencephalograms (EEG) analysis. Past and recent work in animal models using neurophysiology, pharmacology, molecular biology and optogenetics has expanded our understanding of the functional neuroanatomy and synaptic connectivity of sleep circuits.[7–9] Unfortunately, in humans, the underlying neural circuits important for controlling sleep and wakefulness remain poorly understood.

Parkinson's disease (PD) is highly comorbid with a range of sleep disorders.[10 11] PD is characterised by the loss of dopaminergic (DA) neurons of the substantia nigra pars compacta (SNc) and depletion of dopamine in the striatum. Motor symptoms, characterised by tremor, rigidity and bradykinesia become manifest following a 50%–70% loss of SNc DA neurons, leading to the diagnosis of PD.[12 13] Following dopamine repletion treatment, PD subjects with significant motor fluctuations and dyskinesia are considered for subthalamic nucleus (STN) deep brain stimulation (DBS).[14–17] Although STN-DBS is used to treat motor symptoms, several studies have found that STN-DBS provides benefit for some non-motor symptoms, notably sleep dysregulation through normalisation of sleep architecture.[18–20]

For this study, using local field potentials (LFP) recorded from DBS electrodes implanted in STN, during a full night's sleep in PD subjects, we sought to determine whether unique spectral patterns in STN oscillatory activity would correlate with distinct sleep cycles. We examined the classic designations for oscillatory electrophysiological signals in the brain by frequency band, focusing on the following bands: delta (0–3 Hz), theta (3–7 Hz), alpha (7–13 Hz), beta (13–30 Hz), gamma (30–90 Hz) and high-frequency oscillations (90–350 Hz).[21] LFP recordings provide a unique opportunity to study the activity of otherwise inaccessible deep brain structures in human subjects.[22 23] Of note, the beta band (13–30 Hz) of the LFP spectrum has repeatedly been shown to have greater power in the off-medication and/or off-stimulation state ('off states') relative to on-medication and/or on-stimulation ('on states'), with the converse true for gamma band (30–90 Hz).[24–27] Here, we report on changes in STN-LFP activity across the sleep cycle.

METHODS

Subjects and surgery

This study was approved by the Institutional Review Board of the University of Minnesota, where the surgical and recording procedures were performed. Ten subjects provided informed consent and were enrolled in this study. All study subjects carried a diagnosis of idiopathic PD (table 1). Subjects were unilaterally implanted

To cite: Thompson JA, Tekriwal A, Felsen G, *et al*. *J Neurol Neurosurg Psychiatry* 2018;**89**:95–104.

Table 1 Demographic information, levodopa equivalent daily doses (LEDD) and motor subscales of Unified Parkinson's Disease Rating Scale (mUPDRS). Demographic information for all subjects is provided, as well as LEDD, and motor subscale scores of the mUPDRS, on and off medication, prior to surgery and at the time of the study (3 weeks post-DBS implantation but prior to IPG placement surgery). Note that postsurgery scores were also obtained on and off medication, with electrodes implanted, but not yet connected to IPG (no stimulation)

Patient	Age at surgery	Age at diagnosis	Presurgery UPDRS 'off'	Presurgery UPDRS 'on'	Per cent of improvement (%)	Estimated presurgery LEDD	Postsurgery UPDRS 'off'	Postsurgery UPDRS 'on'	Per cent of improvement (%)
1	70/M	51	44	20	55	1838	39, 36, 38	11, 12, 13	68
2	60/M	49	15	7	53	450	28, 24, 20	7, 9, 9	65
3	68/M	62	18	5	72	1300	34, 43, 25.5	4, 6, 11	80
4	62/F	54	62	33	47	U/A	36, 34, 32.5	4, 6, 5	83
5	58/M	46	39	19	51	1575	24, 25, 21.5	8, 10, 14	55
6	69/F	61	61	24	61	850	31, 24, 31	4, 1.5, 2	91
7	39/M	U/A	44	11	75	1038	31, 34, 33	5, 8, 4	85
8	54/M	U/A	43	9	79	U/A	20.5, 26, 24.5	7.5, 3.5, 12	68
9	61/M	U/A	32	9	72	U/A	22, 26, 20	2, 4, 4	84
10	43/M	U/A	46	16.5	64	600	35, 31, 34	0, 1, 0	99

DBS, deep brain stimulation; F, female; IPG, implanted programmable generator; M, male; U/A, unavailable.

in STN with a quadripolar DBS electrode (model #3389: Medtronic, Fridley, Minnesota, USA) as per routine surgical protocol.[28]

Postoperative recordings

Electrode leads were externalised 3 weeks after DBS macroelectrode implantation, for the 24 hours prior to surgery for implantable pulse generator (IPG) placement. In the evening of the 24 hours recording period, all subjects underwent a polysomnography (PSG) that was timestamped to LFP recordings. Subjects were administered the final daily dose of short-acting DA medications prior to the start of PSG recordings, several hours prior to sleep onset. Subjects were therefore considered to be in the 'off' state. Surgical and LFP recording timelines are depicted in figure 1A. In addition to LFP, other physiological signals, such as bipolar ECG and bipolar forearm electromyography (EMG), were recorded. Subject movements and tremor were also captured with three-axis accelerometers connected to contralateral forearm and foot. Data were then transferred to an offline PC for further analysis.

Video-PSG scoring

Differentiating between wakefulness or a specific sleep state was determined by quantifying the electrophysiological data gathered during video-PSG. Preprocessing steps included band-pass filtering for all EEGs and electrooculography (EOG), from 0.1 to 30 Hz, as well as EMG recordings, from 10 to 500 Hz. As per the 2007 American Academy of Sleep Medicine Guidelines, the following electrode montage was used for sleep evaluation: F3–C3, P3–O1, F4–C4 and P4–O2, LEOG–O2, REOG–O1 and chin EMG.[29 30] Sleep stages were determined by analysing 30 s epochs of the PSG, with each epoch classified as Awake or in one of the following sleep stages: rapid eye movement (REM), or the non-REM (NREM) stages of N1, N2 or N3. Epochs classified as Awake periods were further categorised into 'Awake with movement' (AWM) or 'Awake without movement' (AWOM) based on limb accelerometer activity (figures 2 and 3A, B). The absolute value of the accelerometer output was divided into 30 s epochs, corresponding to those epochs used in classifying the PSG. Epochs that contained threshold crossing deflections categorised as AWM were confirmed through verification of video-PSG data.

Signal analysis and statistics

Signals were analysed using MATLAB V.R2016a (Mathworks, Natick, Massachusetts, USA). Preprocessing consisted of high-pass filtering of LFPs at a cut-off frequency of 1 Hz to remove the DC offset. Notch filtering was also executed at 60 Hz and its harmonics to remove power line noise. After preprocessing, the four LFP channels (0, 1, 2 and 3) were then converted into three bipolar derivations (LFP01, LFP12 and LFP23) by sequentially referencing them. To visualise spectral changes in the signal over time, spectrograms for each subject were generated. Each of these signals was divided into 30 s windows with 15 s overlap. In each 30 s window, the power spectral density (PSD) was estimated using a Fast Fourier Transform from a 2 s long sliding window (Hamming) with 1 s overlap. Each 2 s segment which had energy five times larger than the median of energy of all segments was deemed artefactual and excluded from spectral analysis. In total, 414 out of 8609 (5%) epochs were removed. The final PSD estimate for a 30 s window was calculated as the mean of the artefact-free estimates. Remaining corrupted time bins in the spectrogram, due to long-lasting artefacts, were removed and then interpolated linearly by using the adjacent two bins. The final time-evolving spectra had 15 s time and 0.5 Hz frequency resolution. For each subject, LFP data selected for further analysis were based on which contact was used for therapeutic stimulation, which has been show to correlate with spectral strength of the beta band (13–30 Hz).[31] This was selected as the primary criterion because of the documented high-signal intensity of beta power recorded from STN of off-state PD subjects.[27] A stair plot indicating Awake or sleep stage was overlaid on the spectrogram, allowing for visualisation of changes in LFP spectral power with respect to arousal or sleep state (Figures 2 and 3A, B). To visualise and display epoch classification as AWM or AWOM, the PSG stair plot was overlaid on a plot of accelerometer activity (figure 2).

The PSG-indexed 30 s epochs derived from the bipolar LFP recording were then grouped according to sleep stage. Quantitative analysis of the spectral content for epochs was performed by extracting the frequency band power of the same time segment. We averaged along the time corresponding to the sleep segment and frequency corresponding to the frequency band of interest. Percentage of max band power, rather than raw band power, was used to control for inherent intersubject differences in recorded

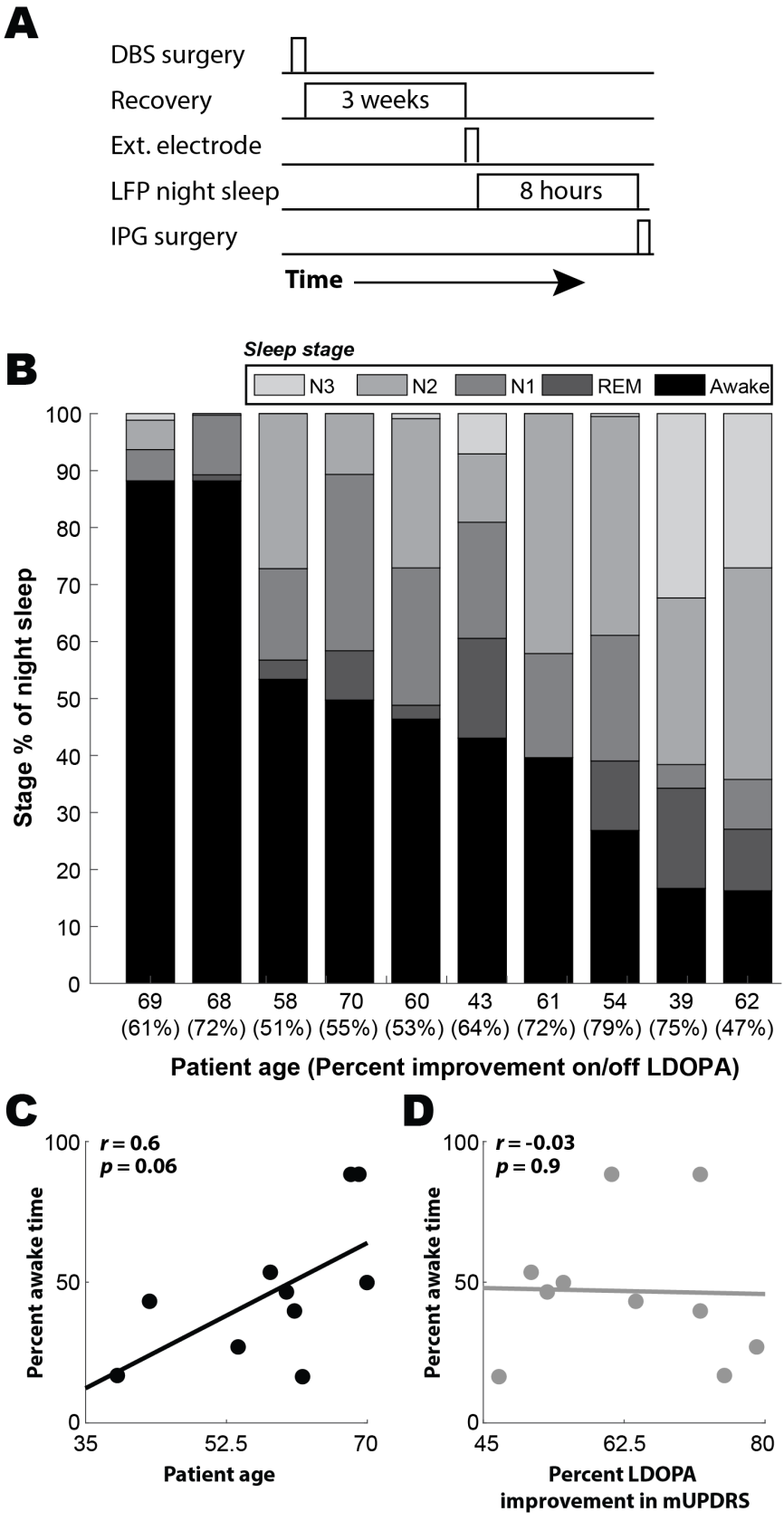

Figure 1 (A) Diagram of timeline for DBS surgery, externalisation of electrode, experimental LFP recordings and surgery for implantation of the IPG. (B) Stacked bar chart representing the proportion of subject sleep cycle as a function of total sleep for each individual subject, sorted from highest to lowest proportion of 'Awake'. For each subject, demographic data for age and per cent improvement on mUPDRS (presurgery on/off LDOPA) are aligned on the X-axis. (C) Correlation between per cent wakefulness and age: r=0.6, p=0.06. (D) Correlation between per cent improvement on/off LDOPA on mUPDRS: r=−0.03, p=0.9. DBS, deep brain stimulation; IPG, implanted programmable generator; LDOPA, levodopa; LFP, local field potentials; mUPDRS, motor subscale of Unified Parkinson's Disease Rating Scale; N1, non-REM stage 1; N2, non-REM stage 2; N3, non-REM stage 3; REM, rapid eye movement.

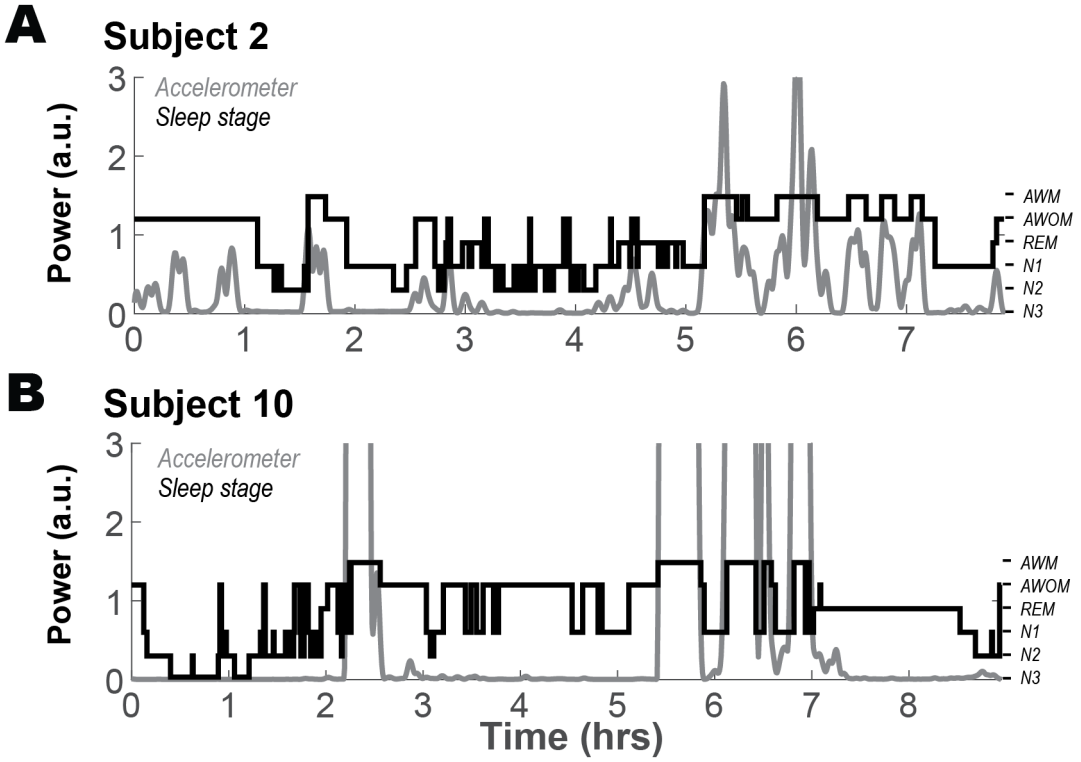

Figure 2 (A) Limb accelerometer data (grey line) were used to classify whether an 'Awake' state coincided with movement, allowing differentiation between AWM and AWOM states. Polysomnography (PSG) data are depicted by a stair plot (black line). PSG-defined sleep stage classifications or Awake state are indicated on the right-hand Y-axis, as AWM, AWOM, REM, N1, N2 and N3. Large deflections in accelerometer recordings correspond to stages scored as AWM. Plot representative of Subject 2. (B) Similar representation to (A) for Subject 10. au, arbitrary units; AWM, awake with movement; AWOM, awake without movement; N1, non-REM stage 1; N2, non-REM stage 2; N3, non-REM stage 3; REM, rapid eye movement.

signal intensity. In addition, to compare between bands across subjects, interband data were scaled using the following normalisation equation:

$$(i) = \frac{x(i) - min(x)}{max(x) - min(x)}$$

where x(i) represents the power in the ith epoch-frequency pair for a given subject.

To quantify spectral change over time, we conducted an analysis to compare the beginning to the end of the LFP recordings. For this analysis, we used the same set of 30 s epochs, but limited to the first 25% and last 25% of the entire recording period for each subject. Within those two quarter blocks, we isolated epochs associated with PSG-defined sleep stages, as described, and computed the per cent of max power for the total spectrum (0–350 Hz).

Predictive model using LFP band power to classify sleep stage: Awake, REM and NREM

To demonstrate that subject-specific frequency band spectral mosaics could be used to predict sleep state, we applied a support vector machine (SVM) classifier model (non-linear—second-order polynomial) to predict the sleep stage identity (Awake, REM and NREM) of each epoch based on the power spectrum data for the five frequency bands (delta, theta, alpha, beta and gamma). For all SVM models, we used a fourfold cross method for validation (25% of the data were left out of the model training). We compared three groups of SVM models: (1) models trained for each subject run on the specific subject, (2) models trained for each subject, but used to predict the sleep epochs of all other subjects and (3) models trained for each subject with pseudorandomly shuffled sleep stage identities for that patient (25 iterations per subject). Mean prediction accuracy (number of correct classifications/total number of classifications) was compared between model groups using a one-way analysis of variance followed by a Tukey's honest significant difference for post hoc comparisons. As further tests of model performance, we generated models for each subject in which each frequency band was left out. Finally, we derived the sensitivity ($true\ positive\ rate = \frac{true\ positives}{true\ positives + false\ negatives}$) and specificity ($true\ negative\ rate = \frac{true\ negatives}{true\ negatives + false\ positives}$) for each of the classified sleep stages (Awake, REM and NREM).

RESULTS

A total of 10 subjects (eight males; age range was 58.4±10.5) with STN-DBS electrodes implanted for the treatment of PD (mUPDRS off: 40.4±15.5; mean±SD), underwent 24 hours combined LFP and PSG recordings, including one full night of sleep (table 1 and figure 1). Of note, in our sample population, when subjects were sorted by greatest proportion of night's sleep represented by wakefulness, we observed trends suggesting that subjects with greater wakefulness were more likely to be older, but did not exhibit differences in improvement in mUPDRS with LDOPA (figure 1C, D; age vs %Awake, r=0.6, p=0.06; %LDOPA improvement vs %Awake, r=−0.03, p=0.9).

Sleep-stage dependent spectral characteristics

Figure 3A and B provide two representative STN LFP spectra recorded during the night. Examination of the relative

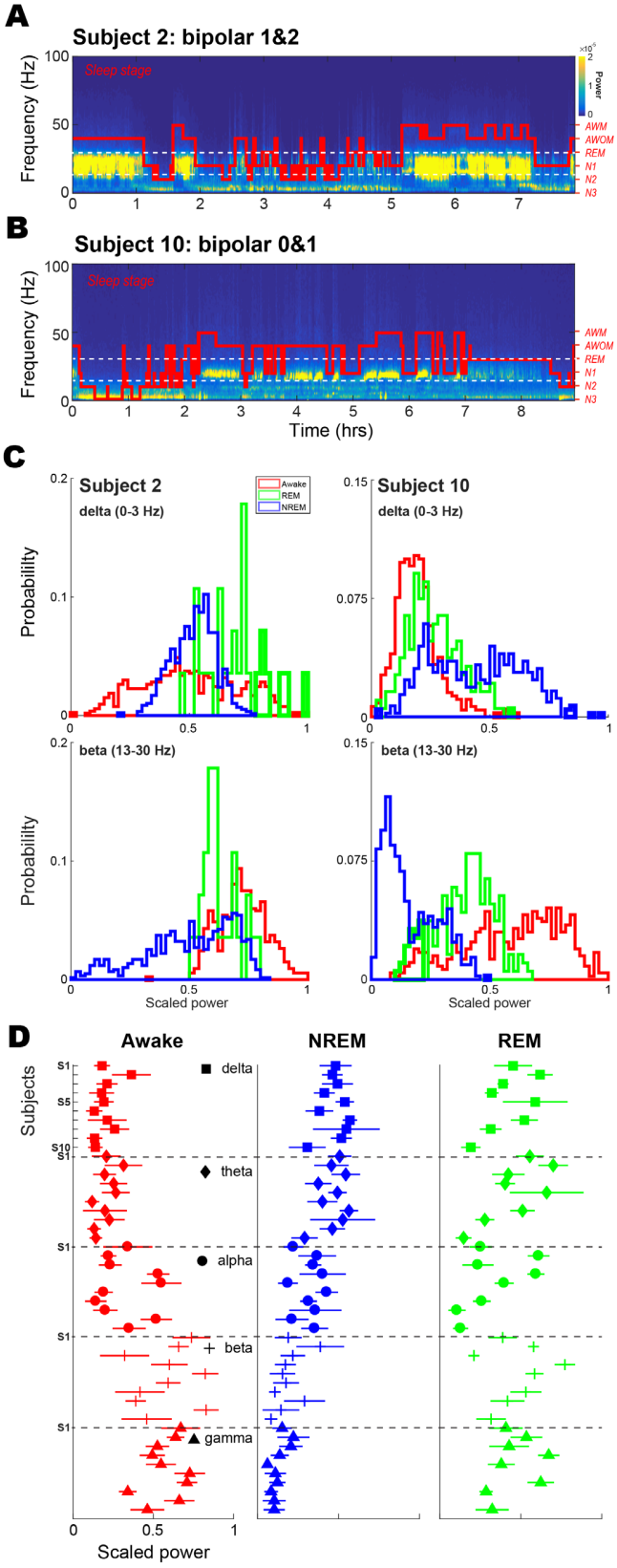

Figure 3 Two representative subthalamic nucleus local field potentials (LFP) spectra recorded during the night. Examination of the relative contribution of each LFP frequency band to sleep stage revealed a striking inverse relationship between the representation of high and low frequency bands, dependent on non-rapid eye movement (NREM) sleep or wakefulness. (C) Representative frequency band power histograms for three sleep states—Awake (combination of AWOM and AWM), NREM (combination of N1, N2 and N3) and REM—from the two subjects depicted in (A) and (B). Both subjects exhibited high delta power during NREM compared with Awake (C, upper panels), whereas beta power was higher in Awake relative to NREM (C, bottom panels). AWM, awake with movement; AWOM, awake without movement; N1, non-REM stage 1; N2, non-REM stage 2; N3, non-REM stage 3; REM, rapid eye movement.

contribution of each LFP frequency band to sleep stage revealed a striking inverse relationship between the representation of high and low frequency bands, dependent upon NREM sleep or wakefulness. Figure 3C shows representative frequency band power histograms for three sleep states – Awake (combination of AWOM and AWM), non-REM (combination of N1, N2 and N3), and REM - from the two subjects depicted in Figures 3A and B. Both subjects exhibited high delta power during NREM compared to Awake (figure 3C upper panels), whereas beta power was higher in Awake relative to NREM (figure 3C bottom panels).

Shared sleep-stage dependent spectral patterns are evident at the individual subject level (figure 3C) as well as at the group level (figure 3D). Indeed, in the Awake column (red), as the band frequency increases there is a concordant increase in proportion of band representation. Conversely, for NREM (blue), across subjects, lower frequency bands exert the greatest influence on power. In both the individual subject histograms (figure 3C) and group data (figure 3D), REM (green) exhibits the greatest variability in representation across the frequency spectra.

Subject-specific patterns in sleep-stage spectral characteristics

Between subjects, variability was noted in terms of the specific frequency band that most significantly distinguished sleep from awake states. Figure 4A illustrates the relative proportion of max power of six different power bands in individual subjects. Stacked bar charts representing the per cent contribution of each frequency band (using the mean) to every stage of sleep for all 10 individual subjects illustrates the unique combinations of spectral features that characterise each subject's sleep architecture (figure 4B). Comparing between subjects reveals that some subjects exhibited similar patterns of sleep architecture at the spectral level, but also that some subjects exhibited sleep stages featuring unique spectral combinations.

Previous work has shown that in PD-STN, beta oscillations fluctuate in response to the administration of LDOPA, movement

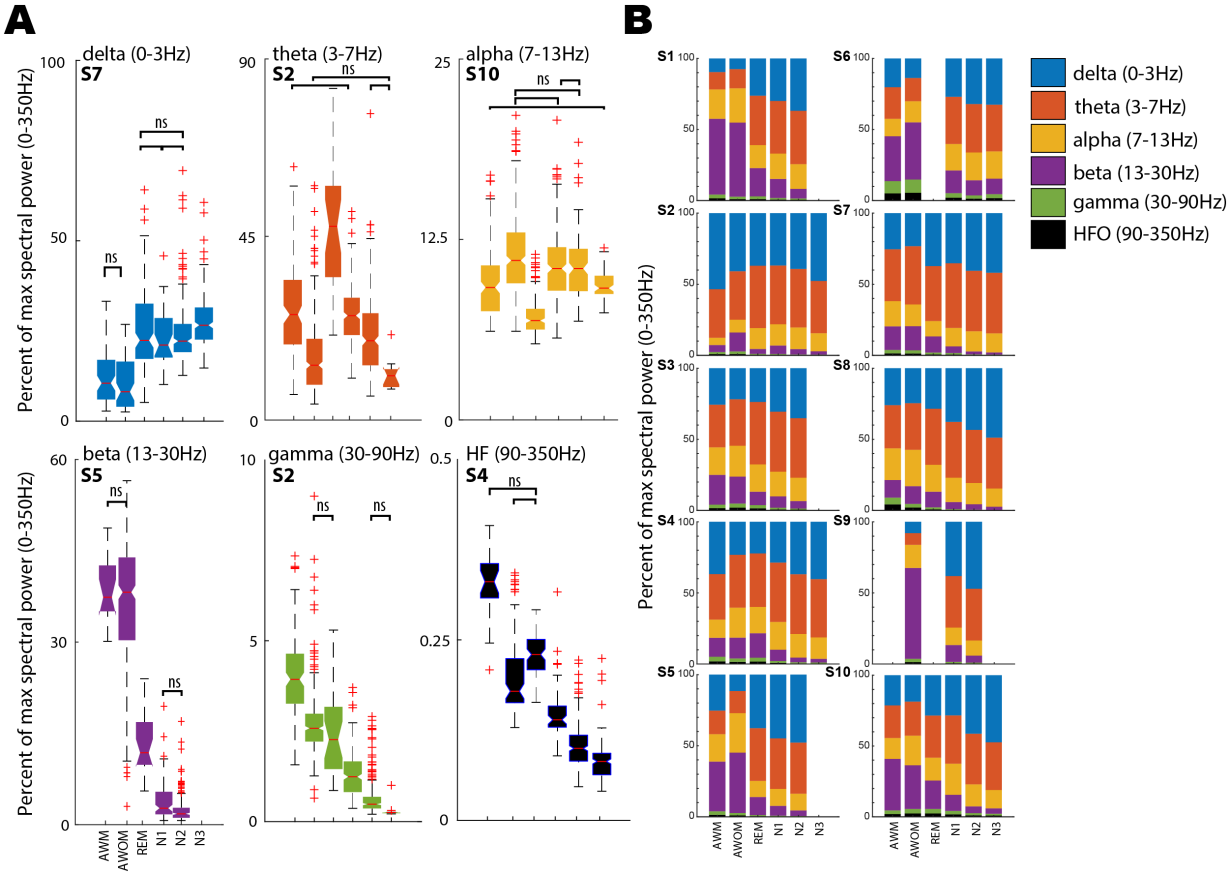

Figure 4 (A) Notched boxed plots comparing the distributions of relative frequency contribution to sleep stage. Each individual plot highlights the contribution of a single frequency band to different stages of sleep for one subject. Mid-box horizontal lines represent median values, with the notch representing the 95% CI for the median. The lower and upper extremes of the boxes represent 25% (Q1) and 75% (Q3) quantiles, respectively. Lower boxplot whisker extends to (Q1–IQR*1.5) and upper boxplot whisker extends to (Q3+IQR*1.5). Values falling outside of this range are identified as plus signs. Within each band, sleep stage differences were compared with a Kruskal-Wallis H test and post hoc comparisons were derived with a Dunn's test: delta, Subject 7, $\chi^2(5)=256.79$, $p=1.9\times10^{-53}$; theta, Subject 2, $\chi^2(5)=338.85$, $p=4.4\times10^{-71}$; alpha, Subject 10, $\chi^2(5)=389.23$, $p=6.2\times10^{-82}$; beta, Subject 5, $\chi^2(4)=517.34$, $p=1.2\times10^{-110}$; gamma, Subject 2, $\chi^2(5)=871.43$, $p=4.1\times10^{-186}$; high-frequency oscillations, Subject 4, $\chi^2(5)=476.84$, $p=7.9\times10^{-101}$. (B) Stacked bar plots, for each subject, depict median power values for all frequency bands and highlight the diversity of spectral contribution to different sleep stages. Values represent the proportion of max band power observed (0–350 Hz) for the respective sleep stage. For example, band power of 13–30 Hz and of 30–350 Hz is a smaller percentage of max spectral power of N3 than it is of REM. AWM, awake with movement; AWOM, awake without movement; N1, non-REM stage 1; N2, non-REM stage 2; N3, non-REM stage 3; REM, rapid eye movement.

and sleep stage[32] and in our subject data, we observed higher variability in beta power. Therefore, we analysed intrasubject beta power—in addition to gamma—over the course of the night to determine whether washout of LDOPA or changes in sleep over the night affected an increase in temporal variation.[32] Beta and gamma band power from the first and final quarter of the PSG-LFP recordings were compared for all subjects. In both representative subjects (Subjects 7 and 10; figure 5A) and group data (figure 5B), significant increases were observed in beta power across all sleep stages (main effect for beta, $\chi^2(5)=2203.98$, $p<0.0001$; post hoc comparisons using Dunn's test: Awake first vs fourth quarter, $p<0.0001$; NREM first vs fourth quarter, $p<0.002$; REM first vs fourth quarter, $p<0.002$). However, gamma exhibited an increase for Awake, but decreases in both NREM and REM (figure 5B; main effect for gamma, $\chi^2(5)=2295.22$, $p<0.0001$; post hoc comparisons using Dunn's test: Awake first vs fourth quarter, $p<0.002$; NREM first vs fourth quarter, $p<0.0001$; REM first vs fourth quarter, $p<0.0004$). This increase in beta power over the course of the night's recording supports a temporal effect consistent with DA medication wearing off and likely had some effect on spectral power in all subjects.

Use of LFP spectrum to predict sleep-stage transitions

To determine whether the spectral content of an individual subject's LFP data could be used to predict their current sleep stage epoch, we used a SVM model based on the 30 s epoch average power spectrum as the predictor variables and the sleep stage identity as the response variable. We used a separate model for each subject, given that the individual differences were likely to predominate shared features among subjects. Figure 6A illustrates that the SVM models trained for each subject performed better on the subject in which they were trained (black dots) than on different subjects (grey dots). In addition, SVM models trained on shuffled predictor variables performed at about chance, indicating that sleep stage spectral profiles were both highly predictive, but subject specific. Subject-specific model prediction accuracy was significantly greater than both the non-specific subject model prediction accuracy and the randomly shuffled sleep stage identity model prediction accuracy ($F(2,25)=79.45$, $p=4.87e-12$; post hoc comparisons: subject specific vs non-specific $p<0.0001$, specific vs shuffled $p<0.0001$, non-specific vs shuffled $p=0.282$).

To determine whether the subject-specific predictive model was dominated by a single frequency band, for each subject, we generated models in which each band was left out. We found that each model still predicted sleep stage with high accuracy ($p=0.95$; figure 6B). This analysis suggests that no single band is required to predict sleep stage.

In addition, we assessed the classification accuracy of each model for the three sleep stages by measuring the specificity (true negative rate) and sensitivity (true positive rate) for each sleep stage separately. We observed a high-specificity measure for all sleep stages (Awake=0.94, REM=0.99, NREM=0.95; figure 6C). Statistical analysis indicated that the models had higher specificity for REM than Awake ($p<0.05$), but the specificity for NREM was not different from Awake or REM ($p=0.99$, $p=0.10$, respectively; $F(2,25)=3.56$, $p=0.044$). We observed a high-sensitivity measure for all sleep stages (Awake=0.93, REM=0.64, NREM=0.94; figure 6D). Statistical analysis indicated that the models had lower sensitivity for REM than Awake and NREM ($p<0.0008$, $p<0.0005$, respectively), and NREM was not different from Awake ($p=0.98$; $F(2,25)=11.10$, $p=2.23e-4$).

DISCUSSION

In this study of LFP recorded from STN DBS during sleep–wake cycles of 10 subjects with PD, we found significant band-power differences in all NREM states compared with REM and Awake stages, in delta (increase in NREM compared with REM), theta (increase), alpha (increase), beta (decrease) and gamma bands (decrease). The existence of a high-fidelity link between changes in sleep–wake states and changes in LFP spectra support the utility of these LFP findings as a biomarker for sleep in PD. The prominent contributions made by lower frequency bands such as delta (0–3 Hz) and theta (3–7 Hz), to max STN LFP band power during NREM sleep stages (N1, N2 and N3) relative to Awake stages, is a notable finding of our analysis because it (1) corroborates EEG characteristics of sleep–wake cycling, such as NREM slow-wave sleep (N3), (2) provides support for the known gating function of thalamocortical circuits and (3) extends published findings from two previous studies reporting differences in thalamic activity during sleep versus awake states (discussed below).[25 33]

To date, only two publications have reported on changes in LFP recordings from thalamus or basal ganglia, in relation to sleep–wake cycling. In the first of these studies, Kempf *et al* described increases in gamma activity (70 Hz) recorded from LFP in ventral intermediate nucleus of thalamus, in two subjects during Awake and REM sleep states relative to slow-wave sleep—similar to our findings in the current study.[34] Second, Urrestarazu *et al* recorded LFP from STN of 10 PD subjects in the off-DA medication state.[25] This analysis focused on beta power because of well-characterised attenuation of this band in response to DA and DBS therapy.[24 35 36] Interestingly, Urrestarazu *et al* described beta power during REM stage as being *greater than or equal to* beta power during awake periods. In contrast, we found beta power to be significantly greater during REM than NREM stages, but on average, REM beta power was *lower* than Awake beta power. As shown in figure 4B, some of our subjects did exhibit greater beta power during REM than Awake or NREM stages, supporting the possibility that the results described by Urrestarazu *et al*, reflect their smaller sample size. In addition, recordings analysed in our experiment were acquired 3 weeks after DBS electrode implantation (vs 2–4 days after surgery by Urrestarazu *et al*) with the former paradigm resulting in minimising the confounding effect of postsurgical oedema on neuronal recordings.[37] In addition, our STN-LFP findings complement other groups' work examining the effect of DBS on PD subject sleep quality.[20] In recently published work from Baumann-Vogel *et al*, STN stimulation was found to improve subjective sleep quality as well as quantitative measures of sleep. However, pattern of sleep-state transitions and REM sleep characteristics remained atypical.[20] Interestingly, the authors report that the more dorsal the STN-DBS contact, the greater the increase in sleep efficiency. This study highlights the need to understand in greater detail how modulation of the STN affects sleep.

These results inform development of a closed-loop DBS system for the treatment of PD. Recent efforts have focused on gating stimulation to beta power during awake states, with promising preliminary reports.[38] Importantly, our findings suggest that gating stimulation to beta power would likely not allow for high-fidelity differentiation between awake and sleep states because of variability in beta during REM.[38] However, NREM stages comprise the greatest proportion (75%–80%) of sleep in the general population. Furthermore, PD subjects commonly suffer from poor sleep quality, leading to the absence of REM entirely, as seen in Subjects 6 and 9 in our study (Figures 1B and

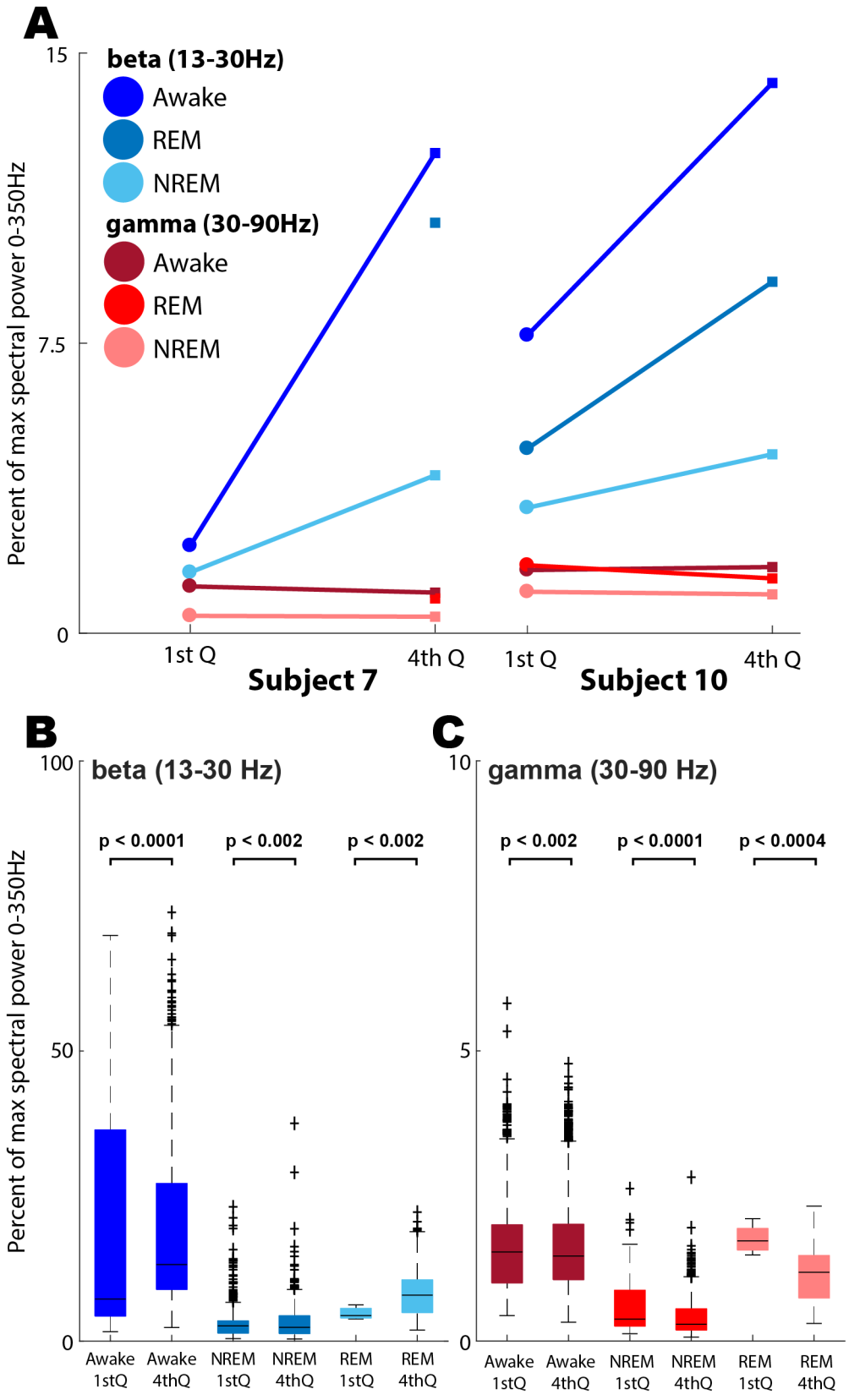

Figure 5 (A) Comparison of beta (13–30 Hz; blue markers) and gamma (30–90 Hz; red markers) power from the first and last quarter of total duration of simultaneous PSG and LFP recording for Subjects 7 and 10, for waking or sleep stage. Subject 7 did not exhibit REM during the first quarter of recorded sleep. Circles and squares represent the mean. (B) Group data for the comparison of beta power over the course of the recording period. In all stages of sleep, across subjects, beta power exhibited an increase over the course of the sleep recording. (C) Group data for the comparison of gamma power over the course of the recording period. Across subjects, gamma exhibited an increase in Awake epochs between the first and last quarters of the recording period, but a decrease in non-rapid eye movement (NREM) and rapid eye movement (REM).

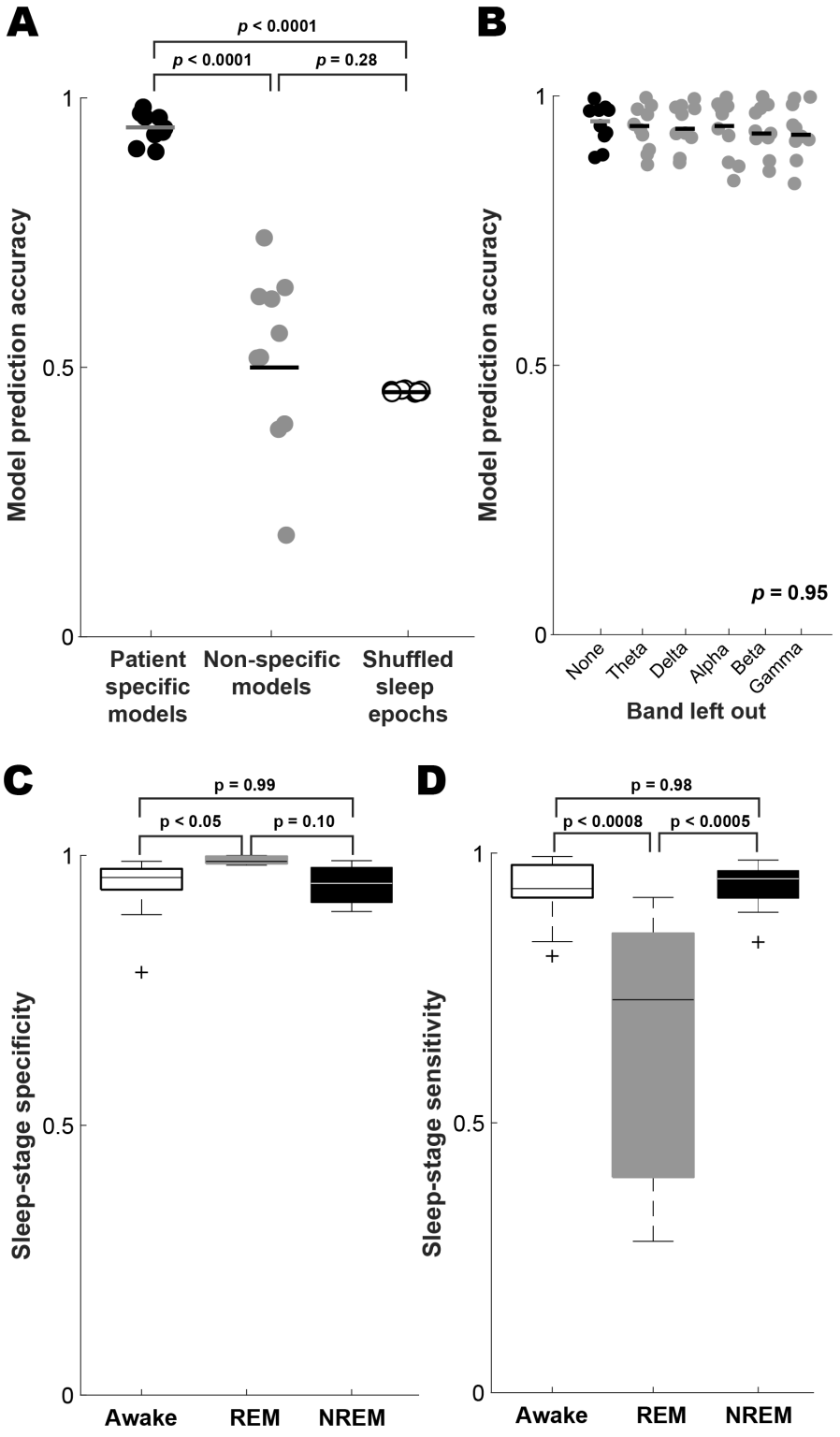

Figure 6 (A) Support vector machine (SVM) models were used to predict sleep stage based on power spectrum profile. The predictor variables were the 30 s binned epochs of average power spectrum data separated into the five frequency bands (delta, theta, alpha, beta and gamma) and the response variable was the hypnogram-defined sleep stage for each epoch. The scatter column plot shows that SVM models trained for each subject performed better on the subject in which they were trained (black dots) and performed poorly when applied to different subjects (grey dots). In addition, SVM models trained on shuffled predictor variables also performed at about chance, indicating that sleep stage spectral profiles were both highly predictive and subject specific. Subject-specific model prediction accuracy was significantly greater than both the non-specific subject model prediction accuracy and the randomly shuffled sleep stage identity model prediction accuracy ($F(2,27) = 79.45$, $p=4.87e{-}12$; post hoc comparisons: subject specific vs non-specific $p<0.0001$, specific vs shuffled $p<0.0001$, non-specific vs shuffled $p=0.282$). (B) Scatter plot representation of individual frequency band contribution to model accuracy for all subject-specific models. For all subjects, models were generated in which each was left out. No individual band was observed to significantly contribute to the overall accuracy of the subject-specific models. (C) Sleep-stage specificity for subject-specific models. (D) Sleep-stage sensitivity for all subject-specific models. NREM, non-rapid eye movement; REM, rapid eye movement.

4B). In our study, intersubject variance confounds using a single frequency band across all subjects that has the statistical power to differentiate consistently between sleep and awake states. Rather, our findings suggest that *for each subject*, individualised analysis is required to identify bands able to fill this role. To this end, we implemented an epoch classification strategy that relies on comparing the spectral mosaics using an SVM classification approach (figure 6). Such analysis would be a natural topic for future studies. Within-subject identification of such a sleep 'footprint' could allow for a closed-loop DBS device to decrease stimulation, and therefore potentially power consumption, during sleep.

LIMITATIONS

Our study is confounded by the fact that a single night of sleep in the hospital is somewhat disturbed relative to the home environment. Future studies could address this confound by recording multiple nights of STN LFP with concurrent PSG, which would also allow us to examine internight variability in subject-specific sleep patterns, although important subject factors make such a study difficult.[39] Additionally, although we converted sometimes complicated home medication regimens into LEDD, and administered a short-acting dopaminergic medication, some subjects had still not transitioned completely to an off-state at the start of PSG sleep recordings. Due to the lack of direct manipulation, there are alternate interpretations of spectral changes over the course nocturnal recording, including, but not limited to: REM intensity, proportion of REM to NREM and the frequency of brief awake interruptions later in the night. However, we believe that contribution of LDOPA washout is a reasonable and parsimonious interpretation. Finally, a fundamental limitation of any study leveraging an invasive technique like DBS is the unavailability of data from a normal control population.

Contributors The study was conceived by AA, NI, JW. Analysis performed by JAT, AT, MO, IT and JW. Data interpretation was performed by JAT, AT, NI and AA. The paper was written by JAT, AT, AA and was edited by all authors.

Funding This research was supported in part by the National Science Foundation, award CBET-1067488, and by a Career Development Award from the National Center for Research Resources to Dr Abosch (5K12-RR03358-03), by an investigator initiated grant from Medtronic (to A.A. and N.F.I.).

Competing interests None declared.

Patient consent Obtained.

Ethics approval Institutional Review Board of the University of Minnesota.

Provenance and peer review Not commissioned; externally peer reviewed.

Data sharing statement Requests for access to data should be addressed to the corresponding author.

REFERENCES

1 Giuditta A, Ambrosini MV, Montagnese P, *et al*. The sequential hypothesis of the function of sleep. *Behav Brain Res* 1995;69:157–66.
2 Pace-Schott EF, Hobson JA. The neurobiology of sleep: genetics, cellular physiology and subcortical networks. *Nat Rev Neurosci* 2002;3:591–605.
3 Colten HR AB, Altevogt BM. Institute of Medicine (US) Committee on Sleep Medicine and Research. *Sleep disorders and dleep deprivation: an unmet public health problem*. Washington (DC): National Academies Press (US), 2006.
4 Prinz PN. Sleep and sleep disorders in older adults. *J Clin Neurophysiol* 1995;12:139–46.
5 Ferrie JE, Kumari M, Salo P, *et al*. Sleep epidemiology – a rapidly growing field. *Int J Epidemiol* 2011;40:1431–7.
6 Hossain JL, Shapiro CM. The prevalence, cost implications, and management of sleep disorders: an overview. *Sleep Breath* 2002;6:85–102.
7 Weber F, Dan Y. Circuit-based interrogation of sleep control. *Nature* 2016;538:51–9.
8 Saper CB, Chou TC, Scammell TE. The sleep switch: hypothalamic control of sleep and wakefulness. *Trends Neurosci* 2001;24:726–31.
9 Saper CB, Fuller PM, Pedersen NP, *et al*. Sleep state switching. *Neuron* 2010;68:1023–42.
10 Iranzo A, Molinuevo JL, Santamaría J, *et al*. Rapid-eye-movement sleep behaviour disorder as an early marker for a neurodegenerative disorder: a descriptive study. *Lancet Neurol* 2006;5:572–7.
11 Tekriwal A, Kern DS, Tsai J, *et al*. REM sleep behaviour disorder: prodromal and mechanistic insights for Parkinson's disease. *J Neurol Neurosurg Psychiatry* 2017;88:445–51.
12 Dauer W, Przedborski S. Parkinson's disease: mechanisms and models. *Neuron* 2003;39:889–909.
13 Ross GW, Petrovitch H, Abbott RD, *et al*. Parkinsonian signs and substantia nigra neuron density in decendents elders without PD. *Ann Neurol* 2004;56:532–9.
14 Hamani C, Saint-Cyr JA, Fraser J, *et al*. The subthalamic nucleus in the context of movement disorders. *Brain* 2004;127:4–20.
15 Bronstein JM, Tagliati M, Alterman RL, *et al*. Deep brain stimulation for Parkinson disease: an expert consensus and review of key issues. *Arch Neurol* 2011;68:165.
16 Abosch A, Timmermann L, Bartley S, *et al*. An international survey of deep brain stimulation procedural steps. *Stereotact Funct Neurosurg* 2013;91:1–11.
17 Tekriwal A, Baltuch G. Deep brain stimulation: expanding applications. *Neurol Med Chir* 2015;55:861–77.
18 Cicolin A, Lopiano L, Zibetti M, *et al*. Effects of deep brain stimulation of the subthalamic nucleus on sleep architecture in parkinsonian patients. *Sleep Med* 2004;5:207–10.
19 De Cock VC, Vidailhet M, Leu S, *et al*. Restoration of normal motor control in Parkinson's disease during REM sleep. *Brain* 2007;130:450–6.
20 Baumann-Vogel H, Imbach LL, Sürücü O, *et al*. The impact of subthalamic deep brain stimulation on sleep-wake behavior: a prospective electrophysiological study in 50 Parkinson patients. *Sleep* 2017;40.
21 Fries P. A mechanism for cognitive dynamics: neuronal communication through neuronal coherence. *Trends Cogn Sci* 2005;9:474–80.
22 Thompson JA, Lanctin D, Ince NF, *et al*. Clinical implications of local field potentials for understanding and treating movement disorders. *Stereotact Funct Neurosurg* 2014;92:251–63.
23 Little S, Brown P. What brain signals are suitable for feedback control of deep brain stimulation in Parkinson's disease? *Ann N Y Acad Sci* 2012;1265:9–24.
24 Giannicola G, Marceglia S, Rossi L, *et al*. The effects of levodopa and ongoing deep brain stimulation on subthalamic beta oscillations in Parkinson's disease. *Exp Neurol* 2010;226:120–7.
25 Urrestarazu E, Iriarte J, Alegre M, *et al*. Beta activity in the subthalamic nucleus during sleep in patients with Parkinson's disease. *Mov Disord* 2009;24:254–60.
26 Kühn AA, Kupsch A, Schneider GH, *et al*. Reduction in subthalamic 8-35 Hz oscillatory activity correlates with clinical improvement in Parkinson's disease. *Eur J Neurosci* 2006;23:1956–60.
27 Weinberger M, Mahant N, Hutchison WD, *et al*. Beta oscillatory activity in the subthalamic nucleus and its relation to dopaminergic response in Parkinson's disease. *J Neurophysiol* 2006;96:3248–56.
28 Abosch A, Lanctin D, Onaran I, *et al*. Long-term recordings of local field potentials from implanted deep brain stimulation electrodes. *Neurosurgery* 2012;71:804–14.
29 Iber C, Ancoli-Israel S, Al CJ, *et al*. The AASM manual for the scoring of sleep and associated events: rules, terminology, and technical specification. *Am Acad Sleep Med* 2007.
30 Morgenthaler TI, Lee-Chiong T, Alessi C, *et al*. Practice parameters for the clinical evaluation and treatment of circadian rhythm sleep disorders. An American Academy of Sleep Medicine report. *Sleep* 2007;30:1445–59.
31 Zaidel A, Spivak A, Grieb B, *et al*. Subthalamic span of beta oscillations predicts deep brain stimulation efficacy for patients with Parkinson's disease. *Brain* 2010;133:2007–21.
32 Brown P, Oliviero A, Mazzone P, *et al*. Dopamine dependency of oscillations between subthalamic nucleus and pallidum in Parkinson's disease. *J Neurosci* 2001;21:1033.
33 Kempf F, Brücke C, Salih F, *et al*. Gamma activity and reactivity in human thalamic local field potentials. *Eur J Neurosci* 2009;29:943–53.
34 Kempf F, Brücke C, Salih F, *et al*. Gamma activity and reactivity in human thalamic local field potentials. *Eur J Neurosci* 2009;29:943–53.
35 Little S, Brown P. The functional role of beta oscillations in Parkinson's disease. *Parkinsonism Relat Disord* 2014;20(Suppl 1):S44–8.
36 Qasim SE, de Hemptinne C, Swann NC, *et al*. Electrocorticography reveals beta desynchronization in the basal ganglia-cortical loop during rest tremor in Parkinson's disease. *Neurobiol Dis* 2016;86:177–86.
37 Lempka SF, Miocinovic S, Johnson MD, *et al*. *In vivo* impedance spectroscopy of deep brain stimulation electrodes. *J Neural Eng* 2009;6:46001.
38 Little S, Pogosyan A, Neal S, *et al*. Adaptive deep brain stimulation in advanced Parkinson disease. *Ann Neurol* 2013;74:449–57.
39 Rosa M, Scelzo E, Locatelli M, *et al*. Risk of infection after local field potential recording from externalized deep brain stimulation leads in Parkinson's disease. *World Neurosurg* 2017;97:64–9.